GEOPHYSICAL RESEARCH LETTERS, VOL. 35, L02706, doi:10.1029/2007GL031087, 2008

Generation of hyper climate modes

D. Dommenget[1] and M. Latif[1]

Received 22 June 2007; revised 28 November 2007; accepted 13 December 2007; published 19 January 2008.

[1] It is shown that some important aspects of the space-time structure of multidecadal sea surface temperature (SST) variability can be explained by local air-sea interactions. A concept for "Global Hyper Climate Modes" is formulated: surface heat flux variability associated with regional atmospheric variability patterns is integrated by the large heat capacity of the extra-tropical oceans, leading to a continuous increase of SST variance towards longer timescales. Atmospheric teleconnections spread the extra-tropical signal to the tropical regions. Once SST anomalies have developed in the Tropics, global atmospheric teleconnections spread the signal around the world creating a global hyper climate mode. A simple model suggests that hyper climate modes can vary on timescales longer than 1,000 years. Ocean dynamics may amplify theses modes and influence the regional expression of the variability, but are not at the heart of the mechanism which produces the hyper modes. **Citation:** Dommenget, D., and M. Latif (2008), Generation of hyper climate modes, *Geophys. Res. Lett.*, *35*, L02706, doi:10.1029/2007GL031087.

1. Introduction

[2] Climate variability on multidecadal timescales of many decades has been described extensively from observations of the last millennium [e.g., *Mantua et al.*, 1997; *Delworth and Mann*, 2000; *Latif et al.*, 2004]. Understanding the mechanisms generating the multidecadal climate variability is a prerequisite for an early detection of anthropogenic climate change. Multidecadal climate variability is reflected in many societal important aspects. Hurricane activity in the Atlantic sector, for instance, varies in phase with multidecadal sea surface temperature (SST) variations [*Landsea et al.*, 1999]. Likewise, Sahelian rainfall exhibits similar multidecadal variations [*Folland et al.*, 1986]. Different competing hypotheses were put forward to explain the multidecadal variability. On the one hand, external forcing factors were proposed such as variations in incoming solar radiation [*Stott et al.*, 2000]. On the other hand, mechanisms internal to the coupled ocean-atmosphere system were used to explain the multidecadal climate variability [*Delworth et al.*, 1993; *Latif and Barnett*, 1994; *Latif et al.*, 2006].

[3] In this study we analyse global-scale climate variability on multi-decadal to centennial timescales. Based on observations, model simulations and a simple conceptual model we illustrate some similarity in the global spatial structure and timescale behaviour in the extra-tropics, leading to the formulation of a theory for "Global Hyper Climate Modes" as forced by local air-sea interaction and the oceans heat capacity.

2. Spatial Structure

[4] The observed pattern of the multidecadal climate variability is obtained from a statistical analysis of global SSTs for the period 1870–2004 using Empirical Orthogonal Functions (EOFs) taken from the HADISST data set [*Rayner et al.*, 2003]. We removed an estimate of anthropogenic climate change from the data by subtracting a fitted exponential trend from each grid point prior to the analysis in order to focus on the internal variability of the climate system. Furthermore, a 10 years running mean filter was applied to eliminate higher-frequency variations. The resulting leading mode (Figure 1a) is global in nature and is referred to as a hyper mode (the term 'hyper mode' was first coined by T. Barnett, 1994 personal communications). It is characterised by the well-known pattern of multidecadal variability in the Pacific, with some connections to the Atlantic and Indian Oceans. In particular, the SST anomaly pattern in the Pacific is symmetric with changes of one sign in the Midlatitudes of both hemispheres, and changes of opposite sign in the Tropics. As expected, the corresponding EOF time series is dominated by multidecadal variations, with warm periods in the tropics around the first half of the 20th century and during the last two decades (Figure 1c). Both the Pacific and the non-Pacific regions contribute significantly to the principal component, indicating the truly global nature of the mode.

[5] Since the instrumental SST observations are rather short, we analysed also data from multi-century control integrations with seven state-of-the-art global climate models which were conducted within the framework of the Fourth Assessment Report (AR4) of the *Intergovernmental Panel on Climate Change* (*IPCC*) [2007]. We used only model runs which were long enough to study the multidecadal variability. External forcing factors are not considered in these simulations, so that we can obtain uncontaminated estimates of the internal variability from the model runs. All models were considered together, each with 340 years, in one EOF analysis, which provides a multi-model estimate of the multidecadal climate variability. The model data were linearly detrended to remove model drift and low-pass filtered in the same way as the observations. The models basically reproduce the hyper mode pattern found in the observations in the Pacific and Indian Ocean region, but exhibit some disagreement in the Atlantic region (Figure 1b). Projecting the multi-model pattern onto the observed data-matrix to reproduce the observed PC-1 time series (Figure 1c), yields a correlation of 0.6 with the observed PC, verifying some similarity between the patterns.

[1]Leibniz Institute for Marine Sciences, Kiel, Germany.

0094-8276/08/2007GL031087$05.00

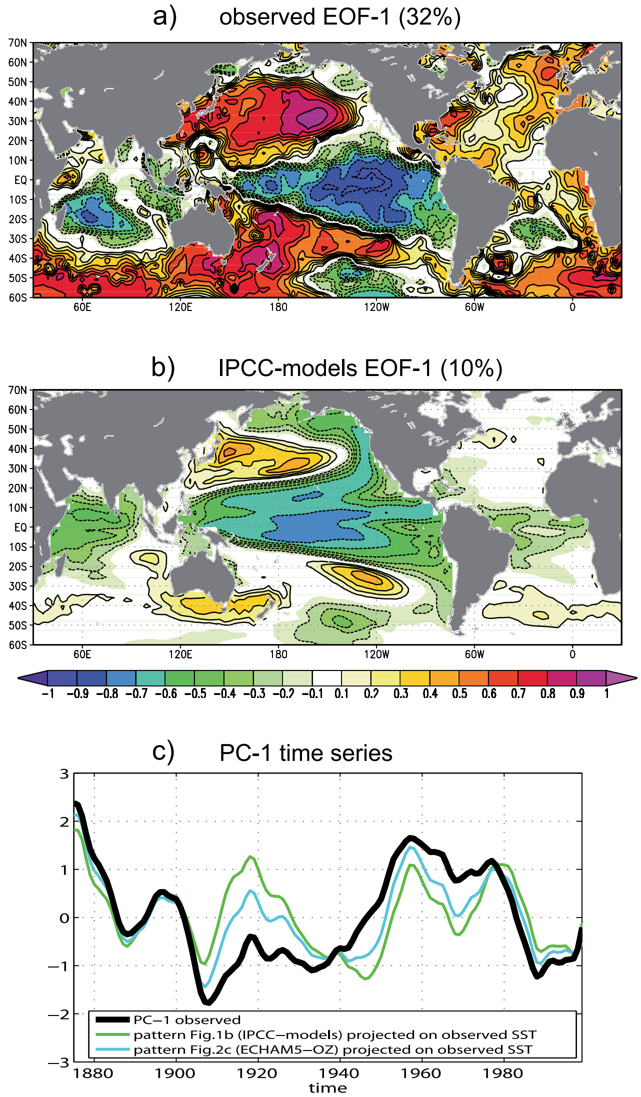

Figure 1. Correlation maps of the leading EOF modes of detrended multi-decadal global sea surface temperatures (SSTs) from (a) the observations and (b) the IPCC multi-model ensemble. (c) The PC-1 time series of the observed SST. For comparison the time series resulting from the projection of the EOF-patterns in Figure 1b and Figure 2c onto the data-matrix of the observed SST are also shown, which illustrates the similarity of the model EOF-patterns with the observed EOF-pattern. The correlations with the PC-1 time series are 0.6 for the IPCC-models and 0.9 for ECHAM5-OZ model, respectively.

[6] Finally, we show the results from a simplified global climate model (ECHAM5-OZ), in which the effects of varying ocean dynamics are not considered (similar to the model of *Alexander and Pendland* [1996]). The atmospheric component of the model ECHAM5 is a state-of-the art general circulation model which is run at horizontal resolution of T31 ($3.75° \times 3.75°$) and with 19 vertical levels. The ocean OZ is represented by 19 vertical layers that are connected through vertical diffusion only. Thus ocean points do not communicate with lateral neighbours. Density depends on temperature and salinity, but density variations are only temperature driven. The ocean is driven at the surface by heat flux and mechanical wind mixing [*Niiler and Kraus*, 1977]. The temperature of the lowest layer at a depth of 500m is restored to the observed climatology. The effects of the time-mean ocean currents are included by a so called Q-flux scheme, which assures a realistic mean state. Changes in ocean currents, however, are not considered. The simplified climate model was integrated for 800 years.

[7] The pattern of the leading EOF-1 of the simplified model is timescale dependent (Figure 2). On interannual timescales (Figure 2a) the leading mode is restricted to the North Pacific. However, when considering longer timescales the leading mode spreads to the equatorial and Southern Pacific, extends beyond the Pacific region and becomes nearly symmetric with respect to the equator on time scales of 40yrs and longer. This suggests that the mode in the North Pacific drives tropical atmospheric teleconnections, which in turn force remote ocean regions, resulting into a coherent global-scale climate mode on longer timescales. Although, there are some important regional differences between the observed pattern and that simulated by the simplified climate model, we conclude that the simplified climate model captures the basic aspects of the hyper mode. In particular, the Pacific anomaly pattern is simulated realistically, and indications of the anomalies in the Atlantic Ocean and the Tropical Indian Ocean are also simulated. The similarity between the observed EOF-1 (Figure 1a) and that of the simplified climate model (Figure 2c) is illustrated by reconstructing the observed PC-1 using the model pattern (Figure 1c), which gives a time series correlation of 0.9. The correlation is still 0.7, if the model pattern only outside the Pacific region is considered. Thus, changes in ocean currents or tropical ocean dynamics seem not to be at the heart of the mechanism that produces the global-scale multidecadal climate variability.

[8] The fraction of explained variance of the leading EOF-1 is quite different in the different data sets, which reflects some problems with the observations and global climate models. The observations are only 13 decades long, which leads to a large uncertainty in the variance and an overestimation of the leading EOFs due to sampling errors. On the other hand the individual IPCC-models produce somewhat different leading EOFs, which results in a relatively small explained variance of the all-model-ensemble leading EOF. Thus we expect that the explained variance of the leading EOF from the simplified global climate model (23%) lies between that of the leading mode of the observations (32%) and that of the multi-model ensemble (10%).

[9] The overall variance of the SST is comparable in all three data sets for most regions of the world, but the IPCC-models have much stronger variability in the extra-tropics.

[10] EOF-1 in the IPCC-models is about 8 times larger than observed, which is related to the much stronger variability in the extra-tropics. The simplified global climate model is missing equatorial variability and has a 4 times larger variance in the EOF-1, which may still be considered within the uncertainty of the observations.

3. Timescales

[11] Next, we compare SST spectra of the extra-tropics in order to get further insight into the nature of the hyper mode

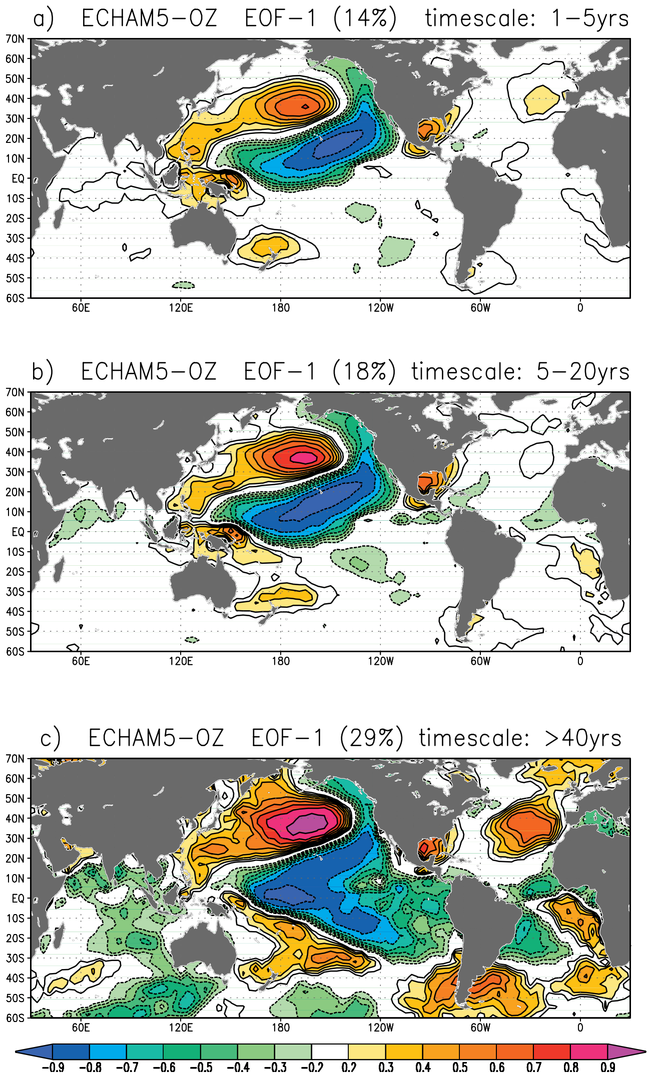

Figure 2. Correlation maps of the EOF-1 of the simple global climate model (ECHAM5-OZ) at different timescales: (a) 1–5 years, (b) 5–41 years, and (c) longer than 41 years.

variability. The mean spectrum of the observed SSTs in the Midlatitudes (Figure 3a) exhibits a red behaviour, with increasing power towards lower frequencies, as expected from the stochastic climate model scenario [*Hasselmann*, 1976]. There are, however, two important deviations from a simple autoregressive model of the first order (AR-1) which was fitted to the data: First, the spectrum does not start to flatten over the timescales analysed, as it does for the fitted AR-1 model. We note that a stationary climate must have a flat spectrum at long periods. Second: The slope of the spectrum is less than ω^{-2}, which was also found by *Dommenget and Latif* [2002] and *Fraedrich et al.* [2004]. The less steep slope has the effect that the relative importance of variances at longer periods is increased if compared to the fitted AR-1 spectrum.

[12] Similar spectra are found in the IPCC-models and the simplified global climate model (Figure 3b) and in the PC-1 of ECHAM5-OZ (Figure 3c). We also note an annual peak in all data sets, despite the fact that the mean annual cycle was removed, which is due to decadal modulations of the annual cycle, as discussed by *Möller et al.* [2008].

[13] Our simplified global climate model can be approximated to zero order by a conceptual model for the upper ocean temperatures:

$$c\frac{dT}{dt} = -\gamma_{surf} \cdot T + \kappa_z \cdot \nabla_z^2 T + \xi_{surf} \tag{1}$$

Here T is the temperature of an upper ocean layer, c is the heat capacity of the ocean layer, and $\gamma_{\rm surf}$ and $\xi_{\rm surf}$ are the damping by the atmosphere and the atmospheric weather forcing, respectively, both of which act only on the surface layer. The latter is considered to have a white frequency spectrum and it is assumed to be independent of T. The vertical diffusion coefficient κ_z is depth dependent.

[14] In a first evaluation of this simple model, we may neglect the finite vertical diffusion and assume a well mixed layer. Then this model reduces to a simple AR-1 model, with the spectrum of the temperature, Γ (ϖ), given by a Fourier transform

$$\Gamma(\varpi) = \frac{\xi_{surf}^2}{\gamma_{surf}^2 + c^2\varpi^2} \tag{2}$$

From this we can understand why the spectra obtained from both the observations and the simplified global climate model increase well into the centennial timescales. The atmospheric damping $\gamma_{\rm surf}$ in relation to the heat capacity c controls the timescale at which the spectrum will flatten. A larger heat capacity c leads to reduced variance on the shortest periods and leaves the variance on the longest periods unchanged. The damping $\gamma_{\rm surf}$ controls the timescale on which the spectrum flattens. On seasonal to interannual timescales, $\gamma_{\rm surf}$ is rather strong and of the order of $\gamma_{surf} \approx 20$ W/K/m^2 for extra tropical regions [*Barsugli and Battisti*, 1998]. On longer timescales and for global-scale patterns, the atmospheric damping will reduce considerably to about $\gamma_{surf} \approx 3$ W/K/m^2, which is basically due to long wave radiation to space [*Barsugli and Battisti*, 1998]. This value may be even smaller due to positive feedbacks in the climate system such as ice-albedo or the water-vapour-temperature feedbacks. For a 5000m deep ocean with $\gamma_{surf} = 3$ W/K/m^2, the spectrum will increase until periods of about 10,000 years. Thus the understanding of ocean-atmosphere interaction and the climate feedbacks acting on the hyper climate modes, require rather long simulations.

[15] If we now consider the full model (1) as a multi-layer model with exponentially decreasing diffusivities between the layers, the slope of the spectrum at the surface can deviate considerably from the AR-1 model's ω^{-2} slope. This is shown in Figure 4a which displays ocean temperature spectra at layers of different depths, from an integration of (1) with a 1000m deep ocean, $\gamma_{surf} = 10$ W/K/m^2 and $\xi_{\rm surf}$ = 30 W/m^2. In particular, the shape of the spectra obtained from the observations and the simplified global climate model (Figure 3) can be mimicked nicely in such a conceptual multi-layer model (Figure 4b). Thus the vertical

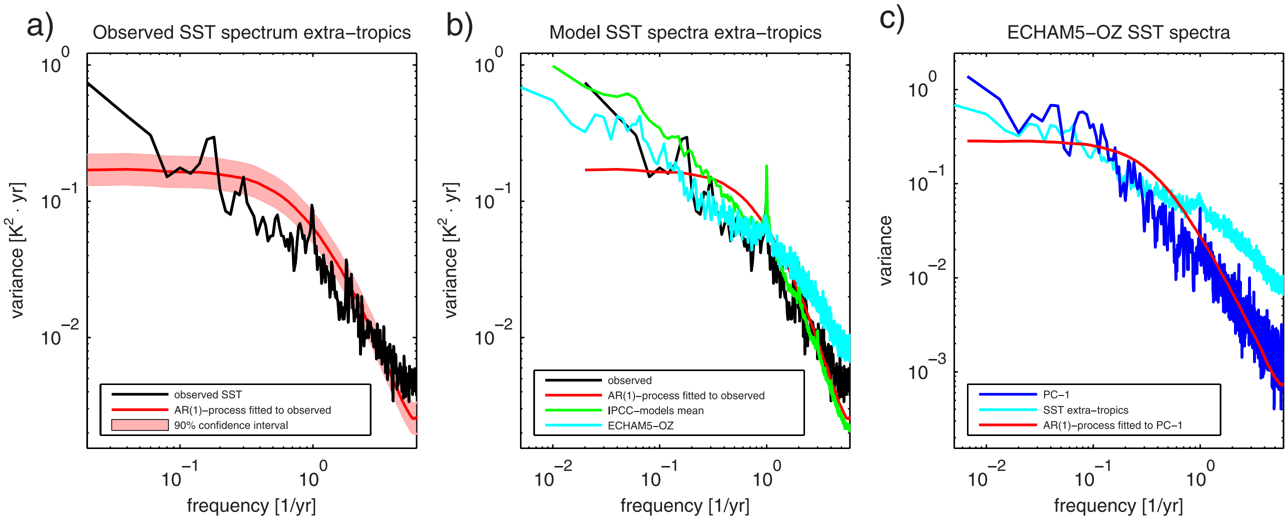

Figure 3. (a) The mean spectrum of observed midlatitudinal SSTs. The spectrum is averaged over all grid points in the North Pacific and North Atlantic Oceans between 30°N and 55°N. (b) Spectra of simulated midlatitudinal SST. (c) Spectrum of PC-1 of the ECHAM5-OZ simulation from the EOF-analysis shown in Figure 2c compared with the mean spectrum of midlatitudinal SSTs and a fitted red noise (AR(1)) process.

profile of the diffusion coefficient κ_z determines the shape of the spectrum, which has an influence on the relative importance of variability at longer time scales.

4. Discussion

[16] Some important characteristics of the spatial structure and timescale behaviour of hyper modes can be simulated within the framework of local air-sea interactions and the upper ocean's heat capacity. A simple climate model suggests the following elements: (1) On seasonal to decadal timescales, regional or basin scale modes of variability exist in the different oceans, which are forced by the atmosphere, ocean dynamics or coupled ocean-atmosphere interactions. (2) The extra-tropical modes involve persistent SST variability, due to the interaction with the large ocean heat capacity, which can lead to weak but persistent forcing of the tropical regions. (3) Once SST anomalies have developed in the Tropics through atmospheric teleconnections [*Barnett et al.*, 1999; *Vimont and Battisti*, 2001], global atmospheric teleconnections spread the signal around the world. (4) Global-scale modes may only be damped by long wave radiation and could be amplified by feedbacks such as water-vapour-temperature and ice-albedo feedbacks. The variance spectrum of this process can increase to timescales longer than 1,000 years and may therefore, in interaction with glacial-feedbacks, potentially be important for ice age cycles.

[17] The questions arises, however, what the role of varying ocean dynamics in the generation of global-scale multidecadal variability is. El Niño-like dynamics [*Neelin et al.*, 1994] will amplify the pattern of the hyper mode in the

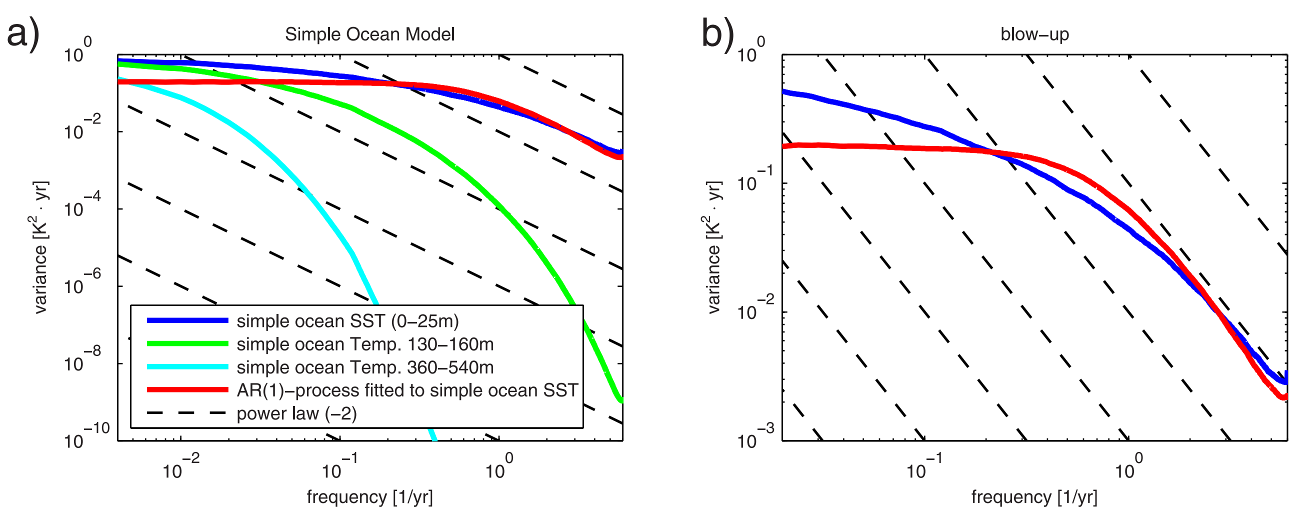

Figure 4. (a) Selected temperature spectra of the conceptual multi-layer model given by equation (1) for different layers. (b) A blow up to ease comparison with the observations shown in Figure 3a. The thin dashed black lines denote the ω^{-2} slope.

equatorial Pacific by the so called Bjerknes feedback [*Neelin et al.*, 1994] on interannual and longer timescales. Changes in wind-induced upwelling may help to amplify the signal of the hyper mode in the southern Tropical Indian Ocean, which may explain the stronger signal in this region in the observations relative to that in our simplified model. There exist, however, multidecadal modes on a regional scale which are driven by deeper ocean dynamics. One prominent example for basin-scale variations in the extra-tropics is the Atlantic Multidecadal Oscillation (AMO) [*Kerr*, 2000] that is forced by variations in the thermohaline circulation [*Latif et al.*, 2004]. Likewise, the variability of the Pacific decadal oscillation (PDO) [*Mantua et al.*, 1997] may be shaped by variations in ocean currents [*Latif and Barnett*, 1994].

[18] The hyper climate mode described here has some similarity with the climate response to increasing green-house gas concentrations as obtained from global climate models, especially in the Pacific. Some global climate models, for instance, simulate an El Niño-like response in the Pacific [*Meehl and Washington*, 1996] very much like the patterns shown in Figure 1. Our analysis indicates that the presence of the hyper mode may make it very hard to detect anthropogenic climate change on a regional scale, as the global change signal and the internal climate variability on multidecadal time scales are not orthogonal.

[19] **Acknowledgments.** This work was supported by the European Unions ENSEMBLES and DYNAMITE Projects. We would like to thank the Max Planck Institute for Meteorology for providing the ECHAM5 model. The integrations were conducted at the German Climate Computing Centre (DKRZ). We thank also the modelling groups who provided the control runs to the WCRP CMIP3 multi-model dataset.

References

Alexander, M., and C. Pendland (1996), Variability in a mixed layer ocean model driven by stochastic atmospheric forcing, *J. Clim.*, *9*, 2424.

Barnett, T. P., D. W. Pierce, M. Latif, D. Dommenget, and R. Saravanan (1999), Interdecadal interactions between the tropics and the midlatitudes in the Pacific basin, *Geophys. Res. Lett.*, *26*, 615.

Barsugli, J. J., and D. S. Battisti (1998), The basic effects of atmosphere-ocean thermal coupling on midlatitude variability, *J. Atmos. Sci.*, *55*, 477.

Delworth, T. L., and M. E. Mann (2000), Observed and simulated multi-decadal variability in the Northern Hemisphere, *Clim. Dyn.*, *16*, 661.

Delworth, T. L., S. Manabe, and R. J. Stouffer (1993), Interdecadal variations of the thermohaline circulation in a coupled ocean-atmosphere model, *J. Clim*, *6*, 1993.

Dommenget, D., and M. Latif (2002), Analysis of observed and simulated SST spectra in the midlatitudes, *Clim. Dyn.*, *19*, 277.

Folland, C. K., T. N. Palmer, and D. E. Parker (1986), Sahel rainfall and worldwide sea temperature 1901–85, *Nature*, *320*, 620.

Fraedrich, K., U. Luksch, and R. Blender (2004), $1/f$ model for long-time memory of ocean surface temperature, *Phys. Rev. E*, *70*, 037301, doi:10.1103/PhysRevE.70.037301.

Hasselmann, K. (1976), Stochastic climate models. Part I: Theory, *Tellus*, *28*, 463.

Intergovernmental Panel on Climate Change (IPCC) (2007), *Fourth Assessment Report*, Cambridge Univ. Press, in press.

Kerr, R. A. (2000), Atlantic climate pacemaker for the centuries, *Science*, *288*, 1984.

Landsea, C. W., R. A. Pielke, A. Mestas-Nunez, and J. A. Knaff (1999), Atlantic basin hurricanes: Indices of climatic changes, *Clim. Change*, *42*, 89.

Latif, M., and T. P. Barnett (1994), Causes of decadal climate variability over the North Pacific and North-America, *Science*, *266*, 634.

Latif, M., et al. (2004), Reconstructing, monitoring, and predicting multi-decadal-scale changes in the North Atlantic thermohaline circulation with sea surface temperature, *J. Clim.*, *17*, 1605.

Latif, M., C. Böning, J. Willebrand, A. Biastoch, J. Dengg, N. Keenlyside, U. Schweckendiek, and G. Madec (2006), Is the thermohaline circulation changing?, *J. Clim.*, *19*, 4631.

Mantua, N. J., S. R. Hare, Y. Zhang, J. M. Wallace, and R. C. Francis (1997), A Pacific interdecadal climate oscillation with impacts on salmon production, *Bull. Am. Meteorol. Soc.*, *78*, 1069.

Meehl, G. A., and W. M. Washington (1996), El Nino-like climate change in a model with increased atmospheric CO_2 concentrations, *Nature*, *382*, 56.

Möller, J., D. Dommenget, and V. Semenov (2008), The annual peak in the SST anomaly spectrum, *J. Clim.*, in press.

Neelin, J. D., M. Latif, and F. F. Jin (1994), Dynamics of coupled ocean-atmosphere models: The tropical problem, *Annu. Rev. Fluid. Mech.*, *26*, 617.

Niiler, P. P., and E. B. Kraus (1977), One dimension models of the upper ocean, in *Modeling and Prediction of Upper Layers of the Ocean*, edited by E. B. Kraus, pp. 143–172, Pergamon, New York.

Rayner, N. A., D. E. Parker, E. B. Horton, C. K. Folland, L. V. Alexander, D. P. Rowell, E. C. Kent, and A. Kaplan (2003), Global analyses of sea surface temperature, sea ice, and night marine air temperature since the late nineteenth century, *J. Geophys. Res.*, *108*(D14), 4407, doi:10.1029/2002JD002670.

Stott, P. A., S. F. B. Tett, G. S. Jones, M. R. Allen, J. F. B. Mitchell, and G. J. Jenkins (2000), External control of 20th century temperature by natural and anthropogenic forcings, *Science*, *290*, 2133.

Vimont, D. J., and D. S. Battisti (2001), Footprinting: A seasonal connection between the tropics and mid-latitudes, *Geophys. Res. Lett.*, *28*, 3923.

D. Dommenget and M. Latif, Leibniz Institute for Marine Sciences, D-24105 Kiel, Germany. (ddommenget@ifm-geomar.de)